UDC 625.7/.8
IRSTI 67.21.17
RESEARCH ARTICLE

THERMAL REGIME OF HIGHWAY SUBGRADES IN SEASONAL FREEZING CONDITIONS OF NORTHERN KAZAKHSTAN

A.S. Sarsembayeva[1], S.T. Mussakhanova[2], Ph. Collins[3]
I.T. Zhumadilov[1], B.C. Kudryshova[2], N.B. Zhuandykov[4]

[1]Shakarim University, Semey, Kazakhstan
[2]Toraighyrov university, Pavlodar, Kazakhstan
[3]College of Engineering, Design & Physical Sciences, Brunel University, London, UK
[4]L.B. Goncharov Kazakh Automobile and Road Academy, 050061, Almaty, Kazakhstan

Abstract. *This study examines the thermal regime of multilayer highway subgrades under seasonal freezing conditions in Northern Kazakhstan, with particular attention to differences between soil beneath the pavement and adjacent snow-covered ground. Field monitoring was conducted along the Kosshy highway near Astana using a vertical array of temperature and relative humidity sensors installed within pavement layers and the underlying soil profile. Measured temperature gradients were used to estimate the effective thermal conductivity of pavement layers and frozen subgrade soil through inverse calculations based on Fourier's law. The results show that the multilayer pavement structure significantly modifies the thermal regime of the soil profile, producing steeper temperature gradients and deeper frost penetration compared with nearby snow-insulated ground. Moisture migration in the vapour phase was evaluated using a diffusion-based formulation derived from Fick's law. In addition, a simplified energy-balance approach was applied to estimate the potential upper limit of vapour-related ice accumulation by relating conductive heat flux to latent heat associated with vapour deposition. The comparison of the pavement and snow-covered profiles demonstrates that differences in thermal conductivity and thermal boundary conditions strongly influence both temperature distribution and potential moisture redistribution in freezing soils.*

Keywords: *vapour transport, frozen soils, road subgrades, frost heave, diffusion method, energy-balance method, heat and mass transfer, pavement*

***Corresponding author**
Saltanat Mussakhanova, e-mail: musaxanova.saltanat@mail.ru

https://doi.org/10.51488/1680-080X/2025.4-19
Received 05 February 2026; Revised 15 February 2026; Accepted 27 February 2026

ӘОЖ 625.7/.8
ҒТАМР 67.21.17
ҒЫЛЫМИ МАҚАЛА

СОЛТҮСТІК ҚАЗАҚСТАННЫҢ МАУСЫМДЫҚ ТОҢДАНУ ЖАҒДАЙЫНДАҒЫ АВТОМОБИЛЬ ЖОЛЫ ЖЕР ТӨСЕМІНІҢ ЖЫЛУ РЕЖИМІ

А.С. Сарсембаева[1], С.Т. Мусаханова[2*], Ф. Коллинз [3], И.Т. Жумадилов[1], Б.Ч. Кудрышова[2], Н.Б. Жуандыков[4]

[1]Шәкәрім университеті, Семей, Қазақстан
[2]Торайғыров университеті, Павлодар, Қазақстан
[3]Инженерия, дизайн және физика ғылымдары колледжі, Брунель университеті, Лондон, Ұлыбритания
[4]Л.Б. Гончаров атындағы Қазақ автомобиль-жол институты, 050061, Алматы, Қазақстан

Аңдатпа. *Бұл зерттеу Солтүстік Қазақстандағы маусымдық қату жағдайындағы көп қабатты тас жол төсемдерінің жылу режимін зерттейді, әсіресе төсем астындағы топырақ пен оған жақын орналасқан қар басқан жер арасындағы айырмашылықтарға назар аударылады. Астана маңындағы Қосшы тас жолы бойында төсем қабаттарына және астыңғы топырақ профиліне орнатылған температура мен салыстырмалы ылғалдылық сенсорларының тік массивін пайдаланып далалық мониторинг жүргізілді. Температура градиенттері өлшенген, төсем қабаттары мен мұздатылған төсем топырағының тиімді жылу өткізгіштігін бағалау үшін Фурье заңына негізделген кері есептеулер арқылы пайдаланылды. Нәтижелер көп қабатты төсем құрылымы топырақ профилінің жылу режимін айтарлықтай өзгертетінін, жақын маңдағы қармен оқшауланған жермен салыстырғанда температура градиенттерінің тік болуын және аяздың тереңірек енуін тудыратынын көрсетеді. Бу фазасындағы ылғалдың миграциясы Фик заңынан алынған диффузияға негізделген формуланы қолдана отырып бағаланды. Сонымен қатар, өткізгіш жылу ағынын будың тұндырылуымен байланысты жасырын жылумен байланыстыру арқылы буға байланысты мұз жиналуының ықтимал жоғарғы шегін бағалау үшін жеңілдетілген энергия балансы тәсілі қолданылды. Жол жабыны мен қар басқан профильдерді салыстыру жылу өткізгіштік пен жылу шекарасы жағдайларының айырмашылығы мұздатылған топырақтарда температураның таралуына да, ылғалдың қайта таралуына да қатты әсер ететінін көрсетеді.*

Түйін сөздер: *бу тасымалы, мұздаған топырақтар, жол негіздері, аяздық ісіну, диффузиялық әдіс, энергетикалық баланс әдісі, жылу және масса алмасу, жол жамылғысы*

***Автор-корреспондент**
Салтанат Мусаханова, e-mail: musaxanova.saltanat@mail.ru

https://doi.org/10.51488/1680-080X/2025.4-19
Алынды 05 ақпан 2026; Қайта қаралды 15 ақпан 2026; Қабылданды 27 ақпан 2026

УДК 625.7/.8
МРНТИ 67.09.33
НАУЧНАЯ СТАТЬЯ

ТЕПЛОВОЙ РЕЖИМ ДОРОЖНЫХ ЗЕМЛЯНЫХ ПОЛОТЕН В УСЛОВИЯХ СЕЗОННОГО ПРОМЕРЗАНИЯ СЕВЕРНОГО КАЗАХСТАНА

А.С. Сарсембаева[1], С.Т. Мусаханова[2*], Ф. Коллинз [3], И.Т. Жумадилов[1], Б.Ч. Кудрышова[2], Н.Б. Жуандыков[4]

[1]Университет Шакарима, Семей, Казахстан
[2]Торайгыров университет, Павлодар, Казахстан
[3]Колледж инженерии, дизайна и физических наук, Университет Брунеля, Лондон, Великобритания
[4]Казахский автомобильно-дорожный институт имени Л.Б.Гончарова, 050061, Алматы, Казахстан

Аннотация. *В данном исследовании изучается тепловой режим многослойных дорожных оснований в условиях сезонного промерзания в Северном Казахстане, с особым вниманием к различиям между грунтом под покрытием и прилегающей заснеженной поверхностью. Полевой мониторинг проводился вдоль шоссе Косшы вблизи Астаны с использованием вертикальной решетки датчиков температуры и относительной влажности, установленных в слоях покрытия и нижележащем грунтовом профиле. Измеренные температурные градиенты использовались для оценки эффективной теплопроводности слоев покрытия и мерзлого грунта основания с помощью обратных расчетов на основе закона Фурье. Результаты показывают, что многослойная структура покрытия значительно изменяет тепловой режим грунтового профиля, создавая более крутые температурные градиенты и более глубокое проникновение мороза по сравнению с расположенной рядом заснеженной поверхностью. Миграция влаги в паровой фазе оценивалась с использованием диффузионной формулы, выведенной из закона Фика. Кроме того, был применен упрощенный подход энергетического баланса для оценки потенциального верхнего предела накопления льда, связанного с паром, путем соотнесения теплопроводности с скрытой теплотой, связанной с осаждением пара. Сравнение профилей дорожного покрытия и снежного покрова показывает, что различия в теплопроводности и тепловых граничных условиях оказывают сильное влияние как на распределение температуры, так и на потенциальное перераспределение влаги в замерзающих грунтах.*

Ключевые слова: *пароперенос, мерзлые грунты, дорожные основания, морозное пучение, диффузионный метод, метод энергетического баланса, тепло- и массоперенос, дорожная одежда*

***Автор-корреспондент**
Салтанат Мусаханова, e-mail: musaxanova.saltanat@mail.ru

https://doi.org/10.51488/1680-080X/2025.4-19
Поступила 05 февраля 2026; Пересмотрено 15 февраля 2026; Принято 27 февраля 2026

ACKNOWLEDGEMENTS/SOURCE OF FUNDING

The study was conducted using private sources of funding.

CONFLICT OF INTEREST

The authors state that there is no conflict of interest.

During the preparation of this manuscript, the authors used artificial intelligence tools (ChatGPT) solely for editorial assistance, such as improving phrasing and checking grammar, spelling, and punctuation. All ideas, interpretations, and conclusions are the responsibility of the authors, who take full accountability for the content of the article.

АЛҒЫС / ҚАРЖЫЛАНДЫРУ КӨЗІ

Зерттеу жеке қаржыландыру көздерін пайдалана отырып жүргізілді.

МҮДДЕЛЕР ҚАҚТЫҒЫСЫ

Авторлар мүдделер қақтығысы жоқ деп мәлімдейді.

Мақаланы дайындау барысында авторлар жасанды интеллект құралдарын (ChatGPT) тек редакциялық көмек мақсатында пайдаланды: тұжырымдарды жетілдіру, грамматикалық, орфографиялық және тыныс белгілеріндегі қателерді тексеру үшін. Барлық идеялар, интерпретациялар мен қорытындылар авторларға тиесілі, және олар мақаланың мазмұнына толық жауапты.

БЛАГОДАРНОСТИ/ИСТОЧНИК ФИНАНСИРОВАНИЯ

Исследование проводилось с использованием частных источников финансирования.

КОНФЛИКТ ИНТЕРЕСОВ

Авторы заявляют, что конфликта интересов нет.

При подготовке рукописи авторы использовали инструменты искусственного интеллекта (ChatGPT) исключительно для редакторской поддержки: корректировки формулировок, проверки грамматических, орфографических и пунктуационных ошибок. Все идеи, интерпретации и выводы принадлежат авторам, которые несут полную ответственность за содержание статьи.

1 INTRODUCTION

Kazakhstan is located in a sharply continental climatic zone characterized by long, severe winters and short, hot summers. In the northern and central regions, ground temperatures frequently fall below −20 °C for extended periods, and seasonal freezing may penetrate more than 2–2.5 m into the soil profile. Under such conditions, frost heave represents one of the most important geotechnical challenges affecting transportation infrastructure. Ice lens formation within road subgrades can lead to differential heave, transverse cracking, and pavement deformation, significantly reducing pavement service life and increasing maintenance costs **(Taber, 1930; Konrad et al., 1980; Sturm et al.,1997, Côté et al.,2005)**.

Field observations along highways in the steppe regions of Kazakhstan indicate that frost-related damage is closely related to the thermal regime of the pavement–soil system. The accumulation of moisture ahead of freezing fronts and the interaction between freezing depth and soil water content have been widely documented for cold-region road infrastructures **(Teltayev et al., 2022; Sarsembayeva et al.,2022)**. Monitoring studies conducted in Kazakhstan also demonstrate that seasonal freezing and thawing processes are strongly influenced by the temperature regime of the upper soil layers and the moisture conditions within the subgrade **(Sarsembayeva et al., 2022; Bragar et al., 2022).** Even relatively small variations in thermal boundary conditions may significantly affect heat and mass transfer processes in freezing soils **(Bragar et al., 2022; Sarsembayeva et al., 2022; Sarsembayeva et al., 2017; Cui et al., 2020).**

The thermal conductivity of pavement and soil layers is a key parameter controlling heat transfer within road structures. Classical predictive models of soil thermal conductivity, such as those proposed by Côté and Konrad **(Côté et al., 2005)**, estimate thermal properties as functions of porosity, mineral composition, and degree of saturation. Laboratory investigations of base materials have shown that dense, moist granular layers may reach thermal conductivities of approximately 1–2 W m^{-1} K^{-1}, whereas more porous asphalt mixtures exhibit substantially lower values **(Sarsembayeva et al., 2017; Sarsembayeva et al., 2015)**. However, multilayer pavement systems represent complex heterogeneous structures in which air-void distribution, contact conditions between layers, and structural heterogeneity may significantly modify effective thermal conductivity compared with theoretical predictions **(Sarsembayeva et al., 2021; Bragar et al., 2022)**.

In addition to conductive heat transfer, moisture migration processes may influence the behaviour of freezing soils beneath road structures. When liquid water mobility is restricted by ice formation, moisture can still migrate through air-filled pores in the vapour phase. This process is commonly described using diffusion-based formulations derived from Fick's law and controlled by temperature gradients and vapour-density differences within the soil profile **(Farouki et al., 1986 Millington et al., 1961)**. Several studies have shown that vapour migration may contribute to moisture redistribution near freezing fronts in unsaturated soils **(Cui et al., 2020; Yu et al., 2018; Murphy et al.,2005)**. Analytical approaches linking measured temperature and relative humidity profiles with vapour flux estimates therefore provide a useful framework for evaluating such processes under field conditions **(Sarsembayeva et al., 2021; Batterman et al.,1996)**.

The present study focuses primarily on the thermal regime of a multilayer highway pavement system and its influence on the underlying soil profile under seasonal freezing conditions. Field monitoring data obtained from the Kosshy highway near Astana were used to analyse temperature distribution beneath the pavement and in adjacent snow-covered ground under natural winter conditions. Effective thermal conductivities of pavement layers and frozen subgrade soil were estimated from measured temperature gradients using Fourier's law. Vapour-phase moisture migration was evaluated using a diffusion-based formulation derived from Fick's law, while a simplified energy-balance approach was applied to estimate the potential upper limit of vapour-related ice accumulation. The objective of the study was to compare heat and mass transfer processes beneath the pavement and in an adjacent snow-covered soil profile during a 126-day freezing period, with particular emphasis on differences in thermal conductivity, temperature gradients, and potential vapour-related ice formation under contrasting surface boundary conditions.

2 MATERIALS AND METHODS

The methodological framework focused primarily on the evaluation of the thermal regime of the pavement–subgrade system and the estimation of effective thermal conductivity of pavement layers and frozen soil from field measurements. Measured temperature gradients were used to assess conductive heat transfer within the multilayer structure. In addition, vapour-phase moisture migration was estimated using a diffusion-based formulation, while a simplified energy-balance approach was applied to obtain an upper-bound estimate of possible vapour-related ice accumulation.

Field monitoring was carried out along the Kosshy highway near Astana, Kazakhstan, an area with a sharply continental climate marked by long winter periods and 120–150 days of subzero temperatures. The road embankment has a multilayer pavement system that includes a 5 cm dense asphalt wearing course, a 10 cm porous asphalt layer, a 12 cm highly porous asphalt base, a 15 cm crushed stone–sand mixture (C-4), a 15 cm gravel–sand bedding layer, and a subgrade of sandy clay (light sandy loam). Along the roadside, a ditch about 0.7 m below the pavement surface accumulated and maintained nearly 0.5 m of snow during the winter season.

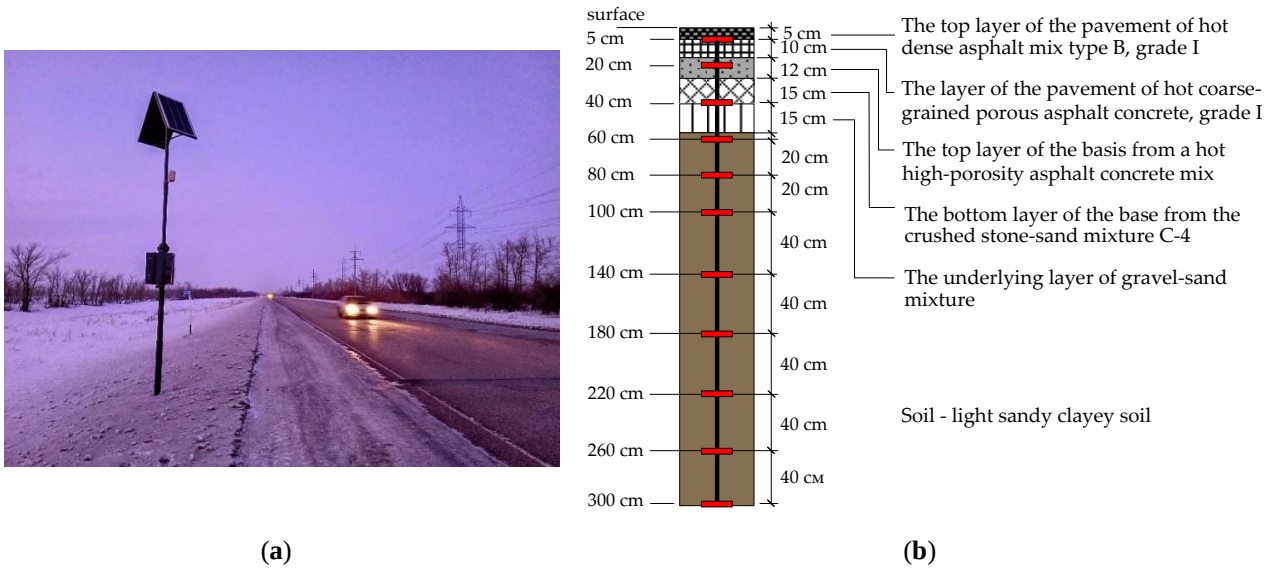

Figure 1 - Monitoring temperature and humidity in pavement layers and under the road: (a) Data logger station; (b) Sensor installation layout (author's materials)

A network of temperature and relative humidity sensors was installed within the pavement structure at predetermined depths of 0, -5, -20, and -40 cm, as well as in the clayey subgrade at 0.4 m spacing intervals **(Figure 1)**. The sensor systems placed beneath the traffic lanes were intended to monitor the coupled thermal and moisture conditions of both flexible and rigid pavements under the combined influence of traffic loading and климатических факторов. In addition, sensor arrays positioned along the shoulder of a cement-concrete section were used to capture cross-sectional variations in the vicinity of embankment slopes and road shoulders **(Aubakirova et al., 2024; Yesbolat et al., 2025).**

At each monitoring location, a combined temperature–humidity probe produced by NPP Interpribor (Chelyabinsk, Russian Federation) was installed. This device consisted of a resistance thermistor together with a dielectric moisture sensor (VIMS-2.2), officially certified in the State Register of Measuring Instruments of the Republic of Kazakhstan. Such an arrangement allowed temperature and relative humidity to be measured simultaneously at the same point within the pavement–subgrade profile.

Throughout the winter period, the sensors continuously recorded temperature (T, °C) and pore-air relative humidity (RH, %), generating an uninterrupted dataset that made it possible to track freez-

ing-front development, vertical temperature gradients, and patterns of moisture migration **(Abdrakhmanova et al., 2025).**

Table 1
Physical and index properties of subgrade soil (averages by depth).

Indicator	1.0 m	2.0 m	2.5 m	3.0 m	4.0 m	6.0 m
Liquid limit wL (%)	22.10	26.80	25.80	27.40	22.40	26.00
Plastic limit wP (%)	10.90	13.50	14.40	15.50	15.30	14.00
Plasticity index IP (%)	11.10	13.30	9.90	11.80	13.00	12.00
Natural water content w (%)	21.00	20.10	17.00	21.80	18.00	20.00
Consistency index IL (–)	0.90	0.53	0.31	0.53	0.39	0.50
Bulk density ρ (g/cm³)	1.78	2.00	2.02	1.99	1.89	2.09
Dry density ρd (g/cm³)	1.47	1.67	1.76	1.66	1.60	1.74
Particle density ρs (g/cm³)	2.72	2.73	2.72	2.72	2.73	2.73
Porosity n (%)	45.92	38.87	36.71	39.85	41.33	36.20
Void ratio e (–)	0.85	0.64	0.57	0.64	0.70	0.57
Degree of saturation Sr (–)	0.67	0.86	0.83	0.89	0.70	0.96

The February 2023 temperature distribution shown in figure 2 reveals pronounced temperature variations close to the pavement surface, but these fluctuations decrease rapidly below a depth of about 0.6 m. This pattern reflects the insulating influence of both the snow cover and the road structure. At greater depths, the temperature curve becomes more uniform and gradually rises toward the unfrozen underlying layer. The point where the profile intersects the 0 °c isotherm indicates the depth of seasonal frost penetration. These observed temperature profiles were later used to inversely determine the thermal conductivity of the individual pavement and soil layers under quasi-steady winter conditions, and also served as the basis for estimating vapour migration and the rate of ice accumulation within the freezing subgrade.

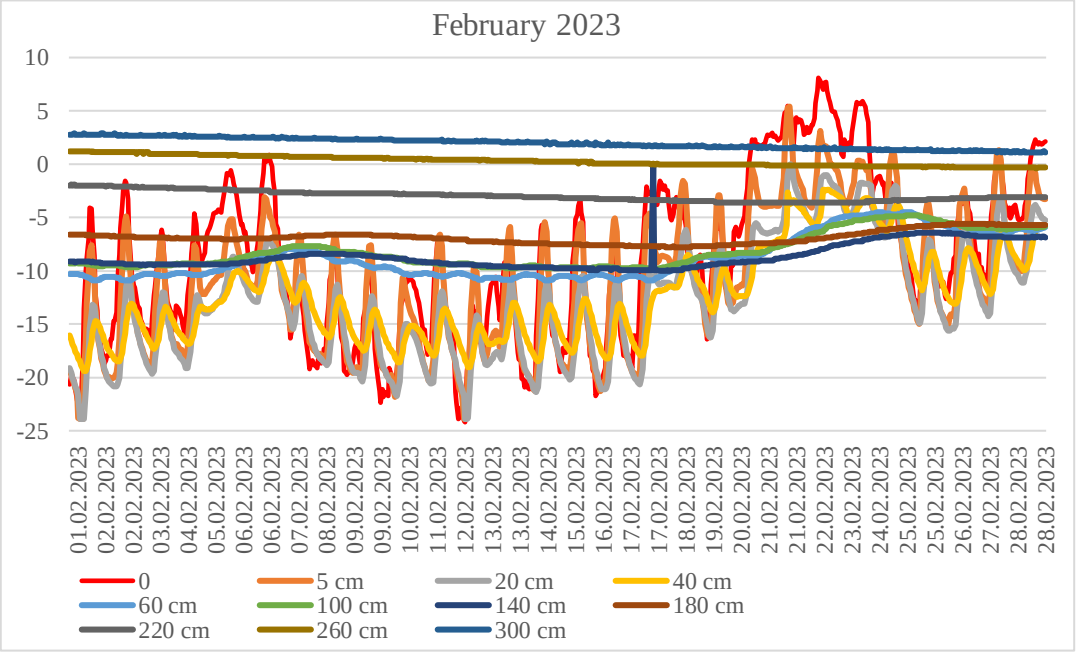

Figure 2 - Temperature regime of the subgrade in February 2023 (author's materials)

Thermal Conductivity section. Thermal conductivity of each pavement layer was back-calculated from the measured midwinter temperature profile by applying Fourier's law for one-dimensional heat conduction under quasi-steady conditions:

$$q = -k\frac{\partial T}{\partial z} \quad (1)$$

where q is the vertical heat flux per unit area (W/m²), calculated from the observed temperature differences ∂T and layer thicknesses ∂z; k is the thermal conductivity of the layer.

This inversion procedure allows estimation of the effective conductive heat flux through the pavement structure and the upper subgrade during the midwinter period when the temperature profile approaches quasi-steady conditions. For the subsequent energy-balance calculations, the total heat energy passing through a layer during a time interval t was determined as:

$$Q = q \cdot t \quad (2)$$

where Q is expressed in J per m², t – time interval in s.

Diffusion-based vapour transport. Moisture transport in the gaseous state was evaluated using Fick's first law of diffusion, but with explicit mass–volume relations to connect measured RH, air volume fraction, and vapour mass flux.

Air-filled pore volume. The volume of air in a 10 cm mould section was computed from air-filled porosity:

$$V_{air} = \theta_a V_{sec} \quad (3)$$

where V_{sec} is the total section volume and L_{sec} its length (0.10 m); A_{air} is the cumulative cross-sectional area of air voids per unit soil section length L_{sec}:

$$A_{air} = \frac{V_{air}}{L_{sec}} \quad (4)$$

The parameter A_{air} represents the total effective area through which vapour migrates in the gaseous phase. Derived from the air-filled porosity (θ_a) and the section volume (V_{sec}), it reflects the cumulative cross-section of all air pores–effectively equivalent to the diameter of an "average" air channel available for vapour flow through the soil.

Vapour density in soil pores.

The instantaneous density of water vapour in pores is:

$$\rho_v = \frac{\mu\, P_s(\mathrm{T})}{RT} RH \quad (5)$$

where ρ_v is the water vapour density calculated from the measured temperature T and relative humidity RH; μ – molar mass of water vapour, P_s(T) – saturated vapour pressure over ice (T ≤ 0 °C) or water (T > 0 °C), R – universal gas constant.

Vapour transport through air pores.

The volume of vapour passing through the air-channel cross-section during time *t* is:

$$V_{vapour} = v \cdot t \cdot A_{air} \quad (6)$$

where v is the mean advective–diffusive velocity in air voids. Combining with mass relation $m_{vapour} = \rho_v \cdot V_{vapour} = \rho_v \cdot v \cdot t \cdot A_{air}$ the velocity is equal to:

$$v = \frac{m_{vapour}}{\rho_v \cdot A_{air} \cdot t} \quad (7)$$

Diffusive vapour flux.

Using Fick's first law, the diffusive mass flux per unit surface area is:

$$J_v^{diff} = -D_{eff} \frac{\partial \rho_v}{\partial z} \tag{8}$$

where J_v^{diff} is the mass flux of vapour (kg·m^{-2}·s^{-1}),

D_{eff} is the effective vapour diffusivity corrected for soil tortuosity:

$$D_{eff} = D_{va}(T) \frac{\theta_a^{4/3}}{\tau} \tag{9}$$

The total vapour flux:

$$J_v^{tot} = J_v^{diff} + J_v^{adv} \tag{10}$$

where $J_v^{adv} = \rho_v u_g$ accounts for advective transport due to gas pressure gradients, u_g is the Darcy gas velocity. In the present study u_g assumed be negligible.

Ice deposition.

The mass of ice deposited at the colder end of each segment during t is:

$$m_{ice} = \rho_v \cdot V_{vapour} = \rho_v \cdot v \cdot t \cdot A_{air} \tag{11}$$

Energy-Balance Method. The second approach provides an approximate upper-bound estimate of vapour-driven ice formation by relating conductive heat flux within the soil to the latent heat associated with vapour deposition. In this simplified formulation, a fraction of the conductive heat flux is assumed to contribute to phase change processes. The parameter α represents the efficiency of conversion between conductive heat transfer and latent heat associated with vapour condensation and freezing. In this study, α = 0.6 was adopted as a representative scenario to illustrate the potential magnitude of vapour-related ice accumulation **(Zhangabay et al., 2025; Nurakhova et al., 2025)**.

Integration and limitations. Both analytical approaches were applied to the same measured temperature and humidity profiles, allowing comparison between diffusion-based estimates and energy-based upper-bound values. The modelling framework assumes one-dimensional vertical heat transfer, quasi-steady winter conditions, negligible gas convection, and homogeneous properties within each soil layer.

3 RESULTS AND DISCUSSION

The measured temperature profile for February 2023 indicates that the soil column remained frozen to a depth of approximately 2.4–2.6 m, while deeper soil layers remained unfrozen. Temperature gradually increased with depth, ranging from approximately −8.9 °C near the pavement surface to about +2 °C at a depth of 3 m. This distribution reflects a persistent upward conductive heat flux from the warmer unfrozen soil layers toward the colder near-surface zone.

A clear difference was observed between the thermal regimes beneath the pavement and beneath the adjacent snow-covered ground. Throughout the entire monitored depth range, the soil beneath the pavement remained significantly colder than the soil beneath the snow cover. At the surface, the temperature under the pavement reached approximately −8.9 °C, whereas beneath the snow cover it was about −7.8 °C. The difference increased with depth and reached its maximum value of about 7 °C at approximately 1.8 m depth.

The snow cover acted as an effective thermal insulator, reducing heat loss from the ground surface and maintaining a relatively warmer and smoother temperature profile. In contrast, the pavement structure intensified surface cooling and promoted stronger vertical temperature gradients within the underlying soil.

The steepest temperature gradients occurred in the lower part of the seasonal frozen layer, particularly within the 1.8–2.6 m depth interval. In this zone, the temperature gradient exceeded approximately 8–9 °C m^{-1}, indicating the presence of strong thermal forcing near the boundary between frozen and unfrozen soil. These gradients play an important role in controlling conductive heat transfer and may also influence vapour-phase moisture migration within the soil profile.

Overall, the observations demonstrate that the multilayer pavement structure significantly modifies the thermal regime of the underlying soil compared with natural snow-covered ground. The pavement promotes deeper frost penetration and stronger temperature gradients, whereas the snow cover acts as a thermal buffer that moderates soil temperature variations during the winter period.

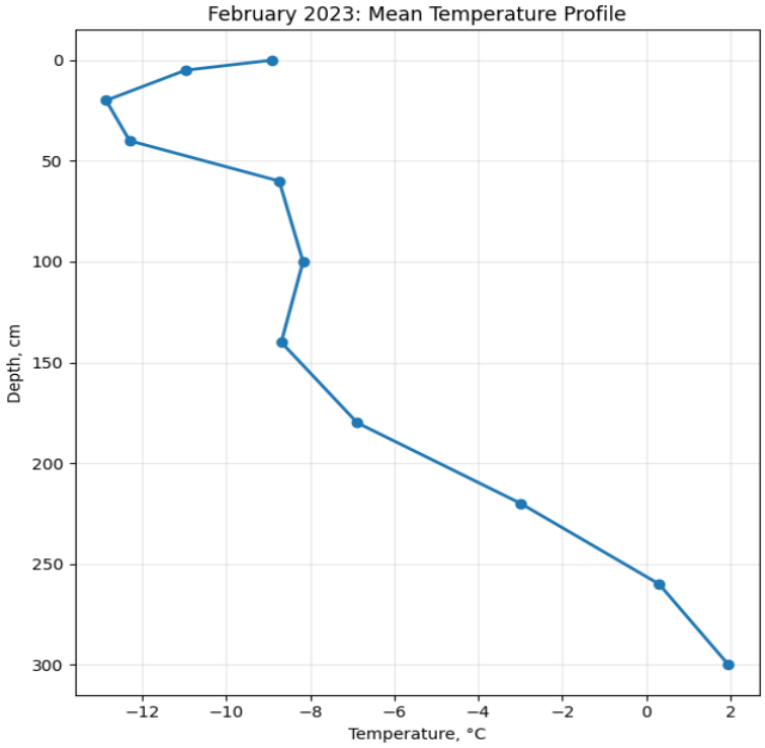

Figure 3 - Temperature distribution beneath the highway pavement (author's materials)

Table 2 summarises the temperature distribution beneath the pavement and in the adjacent natural ground insulated by approximately 0.5 m of snow cover. The measurements show that the pavement profile was consistently colder than the snow-covered profile throughout the entire measured depth range. At the surface, the temperature beneath the snow was −7.8 °C, whereas the pavement surface temperature was −8.9 °C, giving a difference of 1.1 °C. This contrast increased with depth and reached a maximum of 7.0 °C at 1.8 m, where the temperature under snow was 0.1 °C and under the road −6.9 °C.

Below 2.2 m, the difference gradually decreased, although the pavement profile remained colder even at 3.0 m depth, where the temperature difference was still 1.4 °C. These observations confirm that the road structure intensified cooling and promoted deeper frost penetration than the adjacent snow-covered ground. The snow cover acted as a more effective thermal insulator, maintaining a warmer and smoother temperature profile.

Table 2
Temperature distribution across the highway cross-section (February 2023)

Depth (cm)	T under snow (°C)	T under road (°C)	Difference (snow – road), °C
0	−7.8	−8.9	1.1
−5	−7.6	−11.0	3.4
−20	−7.0	−12.9	5.9
−40	−6.1	−12.3	6.2
−60	−5.2	−8.7	3.5
−100	−3.8	−8.2	4.4
−140	−1.9	−8.7	6.8
−180	0.1	−6.9	7.0
−220	1.8	−3.0	4.8
−260	2.9	0.3	2.6
−300	3.4	2.0	1.4

This contrast demonstrates that the pavement structure not only increases surface cooling but also redistributes heat flow within the subgrade, resulting in a colder and deeper frozen zone beneath the road. This difference is important for interpreting the subsequent calculations of thermal conductivity and vapour transport.

The effective thermal conductivity of the pavement layers and the frozen subgrade soil was estimated using inverse calculations based on the measured temperature profile for February 2023 and Fourier's law of one-dimensional heat conduction under quasi-steady winter conditions. The method assumes that, during midwinter, the temperature profile within the pavement–subgrade system approaches a quasi-steady state in which vertical conductive heat transfer dominates.

The back-calculated thermal conductivities for the individual pavement layers are presented in **Table 3**. The results indicate substantial variation in thermal properties between the structural layers of the pavement system. The dense asphalt concrete surface layer exhibited the lowest effective thermal conductivity, reflecting the relatively low thermal conductivity of asphalt mixtures and the presence of air voids within the material.

Table 3
Back-calculated thermal conductivity of pavement system layers.

Layer	Thickness (m)	ΔT (°C)	k (W/m·K)
Dense asphalt concrete	0.05	2.06	0.19
Porous asphalt concrete	0.10	1.26	0.64
Highly porous asphalt	0.12	0.43	2.21
Crushed stone–sand mix	0.15	0.72	1.67
Gravel–sand layer	0.15	2.67	0.45
Frozen sandy clay subgrade	2.43	11.22	1.74

In contrast, the frozen sandy clay subgrade showed the highest thermal conductivity among the analysed layers. The calculated value of approximately 1.7 W m^{-1} K^{-1} is consistent with the expected behaviour of frozen fine-grained soils, where partial ice saturation of pore space significantly increases thermal conductivity. Granular base layers showed intermediate values, reflecting their relatively dense structure and the presence of mineral particles with higher intrinsic thermal conductivity.

The results also demonstrate that the multilayer pavement structure creates a heterogeneous thermal system in which each layer contributes differently to the overall heat transfer through the

pavement–subgrade profile. Layers with lower thermal conductivity act as thermal resistances, while more conductive layers facilitate heat transfer between the surface and the underlying soil.

Using the estimated thermal conductivities and the measured temperature gradients, the conductive heat flux through the pavement–subgrade system during the analysed winter period was calculated to be approximately 10.7 W m^{-2}. This value represents the net upward heat flow from the warmer unfrozen soil layers toward the colder near-surface zone.

The highly porous asphalt yielded a relatively high effective conductivity of 2.21 W m^{-1} K^{-1}, which may reflect the combined effect of its structural connectivity and the inverse character of the calculation based on the measured profile. Overall, the nearly linear temperature gradient in the frozen subgrade supports the assumption that a quasi-steady heat-flow regime was established during the February period analysed.

The obtained heat flux provides an important physical parameter for interpreting moisture migration processes in freezing soils. In particular, it defines the amount of thermal energy available for phase change processes, including vapour condensation and ice formation within the frozen layer. Consequently, the thermal conductivity estimates derived from field measurements serve as a basis for the subsequent evaluation of vapour-phase moisture transport in the soil profile.

The vapour transport analysis was carried out using a diffusion-based formulation derived from Fick's law and incorporating the Millington–Quirk expression for effective gas diffusivity. Vapour density at each monitoring depth was calculated from the measured temperature and relative humidity.

The calculated vapour-density gradients $\frac{\partial \rho_v}{\partial z}$ were positive in most segments, indicating that vapour density increases with depth. As a consequence, the resulting diffusive fluxes are negative, which corresponds to upward vapour migration toward colder layers.

The largest vapour flux beneath the pavement was obtained in the 1.80–2.20 m interval, where the calculated diffusive flux reached -1.62×10^{-9} kg m^{-2} s^{-1}. Slightly smaller magnitudes were obtained in the 1.40–1.80 m and 2.20–2.60 m intervals, confirming that the lower part of the seasonal frozen layer was the main zone of diffusion-driven vapour transport.

Table 4
Diffusion-based vapour flux

Segment (m)	ρ_v^{top}, kg·m⁻³	ρ_v^{bottom}, kg·m⁻³	$\partial\rho_v/\partial z$, kg·m⁻⁴	J_v^{diff}, kg·m⁻²·s⁻¹
0.60–1.00	0.00226	0.00235	2.23×10^{-4}	-6.27×10^{-10}
1.00–1.40	0.00235	0.00238	7.45×10^{-5}	-1.27×10^{-10}
1.40–1.80	0.00238	0.00274	9.08×10^{-4}	-9.63×10^{-10}
1.80–2.20	0.00274	0.00382	2.68×10^{-3}	-1.62×10^{-9}
2.20–2.60	0.00382	0.00495	2.83×10^{-3}	-8.06×10^{-10}

The diffusion-based estimates indicate that vapour movement remained physically consistent but quantitatively small. Even in the most active interval, the calculated daily ice deposition beneath the pavement did not exceed 1.40×10^{-4} kg m^{-2} day^{-1}. These values are too small to explain substantial frost heave by diffusion alone, but they do confirm the presence of a persistent vapour supply toward the colder part of the profile.

For comparison, analogous calculations were performed for the adjacent ground beneath the snow cover. In this case, the vapour-density gradients were smaller and the resulting fluxes were weaker, reflecting the warmer and more gradual temperature profile of the snow-insulated ground.

Table 5
Diffusive vapour flux parameters beneath snow-covered ground

Segment (m)	ρ_v^{top} kg/m³	ρ_v^{bottom}, kg/m³	$\frac{\partial \rho_v}{\partial z}$, kg/m⁴	J_v^{diff}, kg/m²·s
0.60–1.00	0.00303	0.00344	1.02×10^{-3}	-1.91×10^{-10}
1.00–1.40	0.00344	0.00406	1.55×10^{-3}	-1.87×10^{-10}
1.40–1.80	0.00406	0.00482	1.88×10^{-3}	-7.64×10^{-11}
1.80–2.20	0.00482	0.00548	1.66×10^{-3}	-2.50×10^{-11}
2.20–2.60	0.00548	0.00591	1.08×10^{-3}	-1.24×10^{-11}

The weaker vapour fluxes beneath snow indicate that the snow cover substantially reduced the intensity of thermal forcing and thus limited the potential for upward vapour migration. This result is consistent with the warmer temperature regime shown in **Table 2**.

Table 6
Daily ice accumulation predicted by diffusion-based vapour transport (February 2023)

Segment (m)	Under road (kg m⁻² day⁻¹)	Under snow (kg m⁻² day⁻¹)
0.60–1.00	5.42×10^{-5}	1.65×10^{-5}
1.00–1.40	1.09×10^{-5}	1.62×10^{-5}
1.40–1.80	8.32×10^{-5}	6.60×10^{-6}
1.80–2.20	1.40×10^{-4}	2.16×10^{-6}
2.20–2.60	6.97×10^{-5}	1.07×10^{-6}

The largest vapour-driven ice accumulation beneath the pavement occurred in the 1.80–2.20 m layer, corresponding to the strongest vapour-density gradient. In general, the diffusion-based calculations indicate that vapour migration was persistent but quantitatively limited. Even in the most active interval, the predicted daily ice deposition beneath the pavement remained on the order of 10^{-4} kg m^{-2} day^{-1}, whereas beneath the snow-covered ground the values were one to two orders of magnitude smaller. These results suggest that vapour diffusion alone represents only a minor contribution to seasonal ice accumulation, although it confirms the presence of a continuous vapour supply toward colder zones within the frozen profile.

To estimate the potential upper limit of vapour-driven ice formation, a simplified energy-balance approach was applied. In this method, a fraction of the conductive heat flux is assumed to be converted into latent heat associated with vapour deposition and ice formation.

Using the heat flux derived from Fourier's law and assuming $\alpha = 0.6$, the predicted ice deposition rates were substantially larger than those obtained from the diffusion-based approach. Beneath the pavement, the highest deposition was obtained in the 1.80–2.20 m layer, where the predicted value reached 0.3200 kg m^{-2} day^{-1}. A second high value was observed in the 2.20–2.60 m interval, with 0.2711 kg m^{-2} day^{-1}. In the adjacent snow-covered ground, the predicted deposition was more evenly distributed with depth and ranged from 0.0905 to 0.1646 kg m^{-2} day^{-1}.

The energy-balance estimates therefore define an upper envelope of possible vapour-related ice formation under the observed winter thermal regime. In contrast to the diffusion-based results, which remained small throughout the profile, the energy-based approach suggests that the available conductive heat flux may be sufficient to support substantially greater phase-change activity, particularly near the lower boundary of the seasonal frozen layer.

Table 7
Daily ice deposition by the energy-balance method (February 2023, α = 0.6)

Segment (m)	Under road (kg·m⁻²·day⁻¹)	Under snow (kg·m⁻²·day⁻¹)
0.60–1.00	0.0253	0.1152
1.00–1.40	0.0000	0.1564
1.40–1.80	0.1277	0.1646
1.80–2.20	0.3200	0.1399
2.20–2.60	0.2711	0.0905

The analytical framework applied in this study differs from conventional approaches in two principal respects. First, the thermal conductivity of the pavement and subgrade layers was obtained through back-calculation from field-measured temperature gradients using Fourier's law under quasi-steady winter conditions. This inversion procedure yields effective conductivity values that inherently incorporate the heterogeneity of multilayer pavement systems, including differences in asphalt mixtures, granular bases, air-void distribution, and imperfect thermal contact at layer interfaces. Classical predictive models such as those proposed by Côté and Konrad **(Côté et al.,2005)** or Farouki **(Farouki et al., 1986)** estimate soil thermal conductivity primarily as a function of porosity, mineral composition, and degree of saturation. Although such formulations provide useful generalisations, they may not adequately reproduce effective heat fluxes in complex pavement structures where layering and contact resistance strongly influence heat transfer.

The back-calculated thermal conductivities obtained in this study indicate that the frozen sandy clay subgrade exhibits relatively high effective conductivity (approximately 1.7 W m^{-1} K^{-1}), consistent with partial ice saturation of the pore space. The resulting conductive heat flux through the pavement–subgrade system during February was approximately 10.7 W m^{-2}. This value provides an important physical constraint for interpreting vapour migration, because conductive heat transport represents the primary energy source driving phase change and vapour redistribution within the frozen soil profile.

Second, the vapour transport analysis integrates two complementary perspectives: a diffusion-based formulation derived from Fick's law and an energy-balance approach that links conductive heat flux to the latent heat of vapour–ice phase change through an efficiency factor α. The diffusion-based method yielded relatively small but persistent vapour fluxes. Beneath the pavement, the maximum daily deposition rate reached approximately

1.40×10^{-4} kg·m^{-2}·day^{-1} in the 1.80–2.20 m interval, whereas beneath the adjacent snow-covered ground the predicted values were one to two orders of magnitude smaller. When integrated over the frozen depth interval (0.60–2.60 m) and the 126-day freezing season, the cumulative vapour-derived ice mass remains on the order of 10^{-2} kg·m^{-2} beneath the pavement and 10^{-3} kg·m^{-2} beneath the snow-covered ground. These values confirm that diffusion alone represents only a limited mechanism of vapour-driven moisture supply toward the freezing front.

In contrast, the energy-balance approach produces substantially larger estimates because it assumes that a fraction of the conductive heat flux is converted into latent heat associated with vapour condensation and freezing. For the central efficiency scenario with α=0.6, the predicted ice deposition beneath the pavement reaches approximately 0.320 kg·m^{-2}·day^{-1} in the 1.80–2.20 m layer, while the adjacent snow-covered profile yields values between 0.090 and 0.165 kg·m^{-2}·day^{-1} depending on depth. These values exceed the diffusion-based estimates by several orders of magnitude and therefore represent an upper envelope of potential vapour-driven moisture transfer.

Both approaches consistently identify the lower boundary of the seasonal frozen layer as the most active zone of vapour-driven moisture redistribution. In the February profile this zone occurs between approximately 1.8 and 2.6 m depth, where the vertical temperature gradients exceed 8–9 °C m^{-1}. Physically, this region corresponds to the interface between colder frozen soil above and relatively warmer unfrozen soil below, which produces the strongest upward conductive heat flux and the

largest vapour-density gradients. As a result, vapour migration is concentrated near this boundary, where phase change processes can potentially contribute to ice accumulation.

The systematic difference between the pavement and snow-covered profiles further illustrates the role of thermal boundary conditions. The multilayer pavement system produces steeper vertical temperature gradients than the adjacent snow-covered ground because the snow layer acts as an effective thermal insulator. Consequently, the pavement profile supports stronger conductive heat flux and therefore greater vapour migration and potential ice deposition. This behaviour is reflected in the consistently higher vapour-driven ice accumulation predicted beneath the pavement relative to the snow-covered ground.

The magnitude of the calculated vapour fluxes is broadly consistent with previously reported observations. Yu et al. **(Millington, 1961)** reported vapour-driven water fluxes of approximately 0.04–0.14 $kg \cdot m^{-2} \cdot day^{-1}$ during rapid freezing periods, corresponding to about 6–13 % of the total moisture migration. The energy-balance estimates obtained in this study fall within the same order of magnitude, whereas the diffusion-based results are closer to laboratory-derived lower bounds. Batterman **(Batterman, 1996)**, for example, reported effective gas diffusion coefficients corresponding to vapour fluxes on the order of 10^{-6}–10^{-5} $kg \cdot m^{-2} \cdot day^{-1}$ in moist soils. Other studies of frozen soil and snowpack systems **(He et al., 2018; Huang et al., 2023; Zhang et al.,2016)** emphasize the importance of vapour transport in cryogenic processes, although they rarely provide directly comparable daily flux estimates.

Additional context can be obtained from snowpack sublimation studies. Eddy-covariance measurements reported by Reba et al. indicate typical snow sublimation rates of approximately 0.15–0.40 $kg \cdot m^{-2} \cdot day^{-1}$ under sheltered conditions, with episodic values approaching 1–2 $kg \cdot m^{-2} \cdot day^{-1}$ in exposed environments. The upper-bound energy-balance flux obtained in this study (≈0.10–0.32 $kg \cdot m^{-2} \cdot day^{-1}$ depending on depth) therefore lies within the lower envelope of reported snowpack vapour fluxes. This agreement is physically plausible because snow represents a highly porous medium that facilitates vapour exchange, whereas frozen soils are constrained by lower pore connectivity and limited conductive energy supply.

Taken together, these findings indicate that diffusion-based calculations provide a conservative lower bound for vapour-driven moisture migration, whereas the energy-balance method defines an upper envelope of plausible fluxes controlled by the available conductive heat flux. The true contribution of vapour transport to frost heave processes in highway subgrades is therefore likely to lie between these two estimates and to depend strongly on thermal gradients, soil structure, and the efficiency of heat conversion into phase change.

Overall, the results demonstrate that vapour migration, although unlikely to be the dominant mechanism of frost heave, may contribute to moisture redistribution within the lower part of the seasonal frozen layer. By combining inversion-based thermal conductivity estimation with dual-method vapour flux analysis, the present framework provides a more realistic representation of heat and mass transfer in multilayer pavement systems than approaches relying solely on generalized thermal properties. At the same time, the consistent enhancement of vapour-driven ice accumulation beneath the pavement relative to the snow-covered ground highlights that pavement structures influence not only surface cooling but also the internal redistribution of moisture within freezing soils.

4 CONCLUSIONS

This study presented an analytical framework for evaluating thermal conductivity and vapour-driven moisture transport in freezing highway subgrades using field-monitored temperature and humidity data obtained beneath both pavement and adjacent snow-covered ground.

The main conclusions are as follows.

1. Effective thermal conductivities of pavement and subgrade layers were successfully estimated by back-calculation from measured temperature gradients under quasi-steady winter conditions. These values reflect the actual heterogeneity of the multilayer pavement structure and provide a realistic basis for evaluating conductive heat flux.

2. The pavement profile remained consistently colder than the adjacent snow-covered ground throughout the monitored depth range. The multilayer pavement structure intensified surface cooling, promoted steeper temperature gradients, and resulted in deeper frost penetration, whereas the snow cover acted as an effective thermal insulator.

3. The diffusion-based vapour transport calculations produced relatively small vapour fluxes, with maximum daily ice deposition on the order of 10^{-4} kg m^{-2} day^{-1} beneath the pavement and one to two orders of magnitude lower beneath the snow-covered ground. These results indicate that diffusion alone contributes only limited amounts of vapour-derived ice.

4. The simplified energy-balance approach yielded substantially larger deposition estimates. For $\alpha = 0.6$, the predicted daily ice accumulation beneath the pavement reached up to 0.320 kg m^{-2} day^{-1}, representing an upper-bound estimate of possible vapour-related ice formation under the observed thermal conditions.

5. The most active zone of vapour-related moisture redistribution was located near the lower boundary of the seasonal frozen layer, where the strongest temperature gradients were observed. This indicates that thermal boundary conditions play a key role in controlling both heat transfer and the potential for moisture redistribution within freezing road subgrades.

Overall, the results show that vapour transport should be considered in the interpretation of frost-related processes in multilayer road structures, particularly where strong thermal gradients develop beneath pavements under cold continental climatic conditions.

REFERENCES

1. **Taber, S.** (1930). The mechanics of frost heaving. Journal of Geology, 38, 303–317. https://www.jstor.org/stable/30058950
2. **Konrad, J. M., & Morgenstern, N. R.** (1980). A mechanistic theory of ice lens formation in fine-grained soils. Canadian Geotechnical Journal, 17, 473–486. https://doi.org/10.1139/t80-056
3. **Sturm, M., Holmgren, J., König, M., & Morris, K.** (1997). The thermal conductivity of seasonal snow. Journal of Glaciology, 43, 26–41. https://doi.org/10.3189/S0022143000002781
4. **Côté, J., & Konrad, J. M.** (2005). A generalized thermal conductivity model for soils and construction materials. Canadian Geotechnical Journal, 42, 443–458. https://doi.org/10.1139/t04-106
5. **Teltayev, B., Suppes, E., Tileu, K., & Sarsembayeva, A.** (2022). Freezing and thawing characteristics in highway pavements and subgrade in conditions of Kazakhstan. In Proceedings of the 20th International Conference on Soil Mechanics and Geotechnical Engineering (pp. 3981–3985). Sydney, Australia.
6. **Sarsembayeva, A., Zhussupbekov, A., & Collins, P.** (2022). Heat and mass transfer by vapour in freezing soils. Energies, 15, 1515. https://doi.org/10.3390/en15041515
7. **Sarsembayeva, A., Zhussupbekov, A., & Collins, P.** (2021). Heat and mass transfer in freezing soils. In H. H. Zhu et al. (Eds.), Advances in geoengineering along the Belt and Road (Vol. 230, pp. 11–25). Springer. https://doi.org/10.1007/978-981-16-9963-4_2
8. **Bragar, E., Pronozin, Y., Zhussupbekov, A., Gerber, A., Sarsembayeva, A., Muzdybayeva, T., & Sarabekova, U. Z.** (2022). Evaluation of the strength characteristics of silty-clay soils during freezing–thawing cycles. Applied Sciences, 12, 802. https://doi.org/10.3390/app12020802
9. **Sarsembayeva, A., & Collins, P.** (2017). Evaluation of frost heave and moisture/chemical migration mechanisms in highway subsoil using a laboratory simulation method. Cold Regions Science and Technology, 133, 26–35. https://doi.org/10.1016/j.coldregions.2016.10.010
10. **Cui, Y. J., Xu, X., Mu, B., Ren, X. W., Zhu, J. G., & Zhang, D. X.** (2020). Experimental test and prediction model of soil thermal conductivity. Applied Sciences, 10, 2476.

https://doi.org/10.3390/app10072476
11. **Sarsembayeva, A., & Collins, P.** (2015). Evaluation of frost heave and temperature–moisture migration relationship using a modified laboratory method. In Proceedings of the XVI ECSMGE (pp. 3341–3346). ICE Publishing. https://doi.org/10.1680/ecsmge.60678.vol6.523
12. **Farouki, O. T.** (1986). Thermal properties of soils (Vol. 11). Trans Tech Publications.
13. **Millington, R. J., & Quirk, J. P.** (1961). Permeability of porous solids. Transactions of the Faraday Society, 57, 1200–1207. https://doi.org/10.1039/tf9615701200
14. **Yu, L., Lu, X., Li, D., Li, Y., Dong, J., & Huang, J.** (2018). Liquid–vapor–air flow in frozen soil. Journal of Geophysical Research: Atmospheres, 123, 11565–11584. https://doi.org/10.1029/2018JD028502
15. **Murphy, D. M., & Koop, T.** (2005). Review of the vapour pressures of ice and supercooled water for atmospheric applications. Quarterly Journal of the Royal Meteorological Society, 131, 1539–1565. https://doi.org/10.1256/qj.04.94
16. **Batterman, S.** (1996). Effective gas-phase diffusion coefficients in soils at varying water contents. Environmental Science & Technology, 30(7), 2502–2509. https://doi.org/10.1021/es950014i
17. **Sarsembayeva, A., & Zhussupbekov, A.** (2020). Experimental study of deicing chemical redistribution and moisture mass transfer in highway subsoils during unidirectional freezing. Transportation Geotechnics, 24, 100426. https://doi.org/10.1016/j.trgeo.2020.100426
18. **Harlan, R. L.** (1973). Analysis of coupled heat–fluid transport in partially frozen soil. Water Resources Research, 9(5), 1314–1323. https://doi.org/10.1029/WR009i005p01314
19. **Jame, Y. W., & Norum, D. I.** (1980). Heat and mass transfer in a freezing unsaturated porous medium. Water Resources Research, 16(4), 811–819. https://doi.org/10.1029/WR016i004p00811
20. **Hansson, K., Šimůnek, J., Mizoguchi, M., Lundin, L. C., & van Genuchten, M. Th.** (2004). Water flow and heat transport in frozen soil. Vadose Zone Journal, 3(2), 693–704. https://doi.org/10.2136/vzj2004.0693
21. **Dall'Amico, M., Endrizzi, S., Gruber, S., & Rigon, R.** (2011). A robust and energy-conserving model of freezing variably saturated soil. The Cryosphere, 5, 469–484. https://doi.org/10.5194/tc-5-469-2011
22. **He, Z., Zhang, S., Teng, J., Yao, Y., & Sheng, D.** (2018). Vapour transfer and its effects on water content in freezing soils. Chinese Journal of Geotechnical Engineering, 40(7), 1190–1197.
23. **Zhang, S., Teng, J., He, Z., Yao, Y., & Sheng, D.** (2016). Canopy effect caused by vapour transfer in covered freezing soils. Géotechnique, 66(11), 927–940. https://doi.org/10.1680/jgeot.16.p.016
24. **Huang, X., Wang, M., Shi, Y., Yu, X., & Zhou, Q.** (2023). Numerical study of coupled water and vapor flow, heat transfer, and phase change in frozen soil. Water Resources Research, 59, e2022WR032146. https://doi.org/10.1029/2022WR032146
25. **Reba, M. L., Pomeroy, J. W., Marks, D., & Link, T. E.** (2012). Estimating surface sublimation losses from snowpacks. Hydrological Processes, 26, 3699–3711. https://doi.org/10.1002/hyp.8372
26. **Aubakirova, T. A., Myrzakasymova, Zh. Zh., Pentaev, T. P., & Zhanakova, R. K**. (2024). Control of engineering geodetic works during highway reconstruction. Bulletin of the Kazakh Leading Academy of Architecture and Civil Engineering, 2(92), 7–21. [Avtokölik jolynyñ aumağyn qayta quru kezindegi inzhenerlik geodeziyalyq jumystardy baqylau] https://doi.org/10.51488/1680-080X/2024.2-01 (In Kaz.).
27. **Nurakhova, A. K., & Kiyalbay, S. N.** (2025). Model of thermal balance change in large cities. Bulletin of the Kazakh Leading Academy of Architecture and Civil Engineering, 1(95), 75–186. https://doi.org/10.51488/1680-080X/2025.1-11
28. **Zhangabay, N., Oner, A., Buganova, S., Tursunkululy, T., Utelbayeva, A., & Tashmukhanbetova, I.** (2025). Development of a mathematical model of heat transfer through multilayer enclosing structures. Bulletin of the Kazakh Leading Academy of Architecture and Civil Engineering, 2(96), 148–159. https://doi.org/10.51488/1680-080X/2025.2-14
29. **Yesbolat, A. G., Sunanda, J. D., & Bekturganova, N. Ye.** (2025). Optimization of asphalt concrete properties through modeling. Bulletin of the Kazakh Leading Academy of Architecture and Civil Engineering, 3(97), 137–154. https://doi.org/10.51488/1680-080X/2025.3-10
30. **Abdrakhmanova, K. A., Karacasu, M., Mukasheva, A. S., Tleulenova, G. T., Zhairbayeva, G. A., & Muzdybayeva, T. K.** (2025). Experience of applying field tests of soil in Northern

Kazakhstan. Bulletin of the Kazakh Leading Academy of Architecture and Civil Engineering, 4(98), 93–107. https://doi.org/10.51488/1680-080X/2025.4-06